

Numerical Study of the Roll Decay of Intact and Damaged Ships

Qiuxin Gao and Dracos Vassalos
University of Strathclyde

ABSTRACT

In the paper, a RANS based CFD solver with VOF modeling and SST $k-\omega$ turbulence closure is applied to study the roll decay of intact and damage ships. The numerical approach was first implemented on DTMB 5415 roll decay with forward speed. The computed roll decay history and velocity contour agree well with the measured data. Then, the simulations of roll decays of SSRC Burgundy model in intact and damage conditions were carried out. The sway motion was also computed in the case of damage condition. The present computational results show flooding and sloshing affects roll behavior significantly.

KEYWORDS

Flooding, Roll decay, sway, Intact, Damage, Hydrodynamics

INTRODUCTION

A roll decay test is normally carried out to obtain the roll natural frequency and damping characteristics of the model. These parameters are essential in estimating ship response in calm water and in waves.

Most towing tank roll decay tests are in intact conditions with or without speed (Irvine et al, 2004). Only a few are in damage conditions (Mirfield, 2001).

With the rapid advance of high performance computing (HPC) technology and numerical methodology of Computational Fluid Dynamics (CFD), it is time to study intact and damage roll decay numerically.

Special computational techniques are required to simulate roll decay by RANS due to the feature of transient ship motion. These include deforming mesh, moving mesh and grid interface. There were a few numerical works in the intact condition, (Wilson, 2002, Gao 2010). No computational work was yet published in the damage conditions.

In the paper, the numerical simulations of roll decay in both intact and damage conditions by solving RANS equations are presented. The hydrodynamic roll moment on hull and in the compartment are separated. The influence of

parameters such as KG, with and without sway are investigated. The resulting added moment of inertial and damping are compared. The numerical validations are carried out.

MATHEMATICAL MODELLING

The Reynolds averaged Navier-Stokes (RANS) equations with VOF modeling of free surface and SST $K-\omega$ turbulence closure were solved. The governing equations can be written as below.

$$\nabla \cdot \mathbf{u} = 0 \quad (1)$$

$$\frac{\partial \mathbf{u}}{\partial t} + \mathbf{u} \cdot \nabla \mathbf{u} = -\frac{1}{\rho} \nabla p - \mathbf{g} + \nu \nabla^2 \mathbf{u} \quad (2)$$

$$\frac{\partial}{\partial t}(\rho K) + \nabla \cdot (\rho \mathbf{u} K) = \nabla \cdot (\Gamma_K \nabla K) + S_K \quad (3)$$

$$\frac{\partial}{\partial t}(\rho \omega) + \nabla \cdot (\rho \mathbf{u} \omega) = \nabla \cdot (\Gamma_\omega \nabla \omega) + S_\omega \quad (4)$$

$$\frac{\partial}{\partial t}(r_w) + \nabla \cdot (r_w \mathbf{u}) = 0. \quad (5)$$

Computational domain

The computational domain is a numerical rolling tank with 4 ship lengths long, 10 ship lengths wide and 2 ship length deep. The strategy of moving mesh and grid interface is used to cope with free roll motions.

Boundary condition

Open channel boundary conditions with wave damping were implemented at far field.

Slip wall is imposed on tank wall and wall function is used on hull boundary

Numerical detail

Second order upwinding interpolation for convection was used. SIMPLE algorithm was applied to solve pressure. Geometric reconstruction of volume fraction is used to capture free surface. The hydrodynamic and hydrostatic forces were computed and used to update roll and sway motions by UDF of rigid body motion program

The detail of theory and usage can be found in FLUENT manual.

Parallel computing

The calculations were run on a High Performance Computer (HPC) with 8*130 (nodes) processors provided by Esteem Systems Ltd in partnership with SUN Microsystems (now Oracle).

The machine has a theoretical peak performance of 13 TeraFlops—thirteen thousand billion operations per second.

For a typical roll calculation of 2M cells, it takes roughly 20 hours of clock time for computational time 20 seconds using 16 cores.

TEST CASE

Two test cases were studied, i.e DTMB5415 (Irvine et al 2004) and Burgundy section model (Mirfield, 2001). The numerical verification studies were carried out in the relevant test case. The numerical results and validation of test cases were given below.

DTMB5415 roll decay

The test case was used in Gothenburg CFD workshop 2010. The main features of the roll decay test case of DTMB5415 are given below:

- Bare hull with bilge keels
- Towing condition in calm water
- Sinkage: $s = 2.93 \times 10^{-4}$
- Trim: $t = -3.47 \times 10^{-2}^\circ$
- The model speed is 1.53m/s
- The Froude number is 0.138
- Reynolds number 2.56×10^6
- The initial roll angle is 10 degrees

The hybrid meshes were generated with special care of resolution in the boundary layer and near free surface. In total, 3.1M grids were used. The computed roll decay time record was compared with measurement in Figure 1.

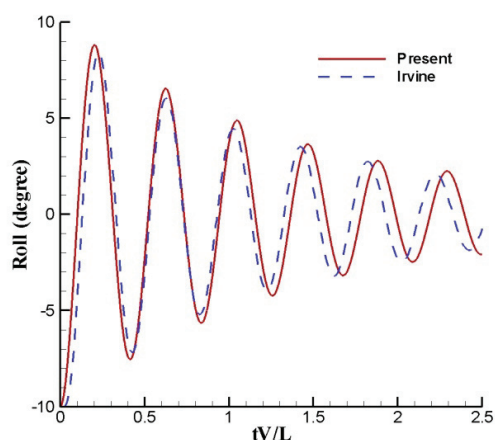


Fig 1: DTMB5415 Roll decay history

The comparison shows that the agreements between calculation and model test are acceptable with slightly larger period and smaller damping from calculation. It seems that KG in the calculation is slightly higher than that in the model test.

The computed and measured longitudinal velocity contours at start of second cycle are shown in Figures 2 and 3. It can be seen that the velocity distributions between calculation and measurement are consistent with boundary layer generally thin on the windside and thick on the leeside of bilge keel.

The numerical validation of DTMB5415 roll decay with sonar dome, transom and bilge keel indicates the numerical accuracy is satisfactory and numerical simulation can be used to study roll damping.

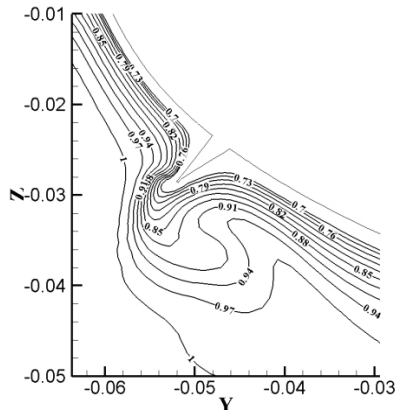


Fig. 2: Computed u contour

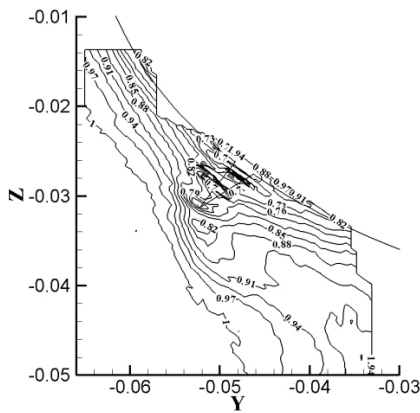


Fig. 3: Measured u contour

Burgundy model roll decay

The test case of burgundy model was used to study roll damping in intact and damage conditions. The main parameters of the model are listed in table 1. The geometry of the model is shown in Figure 4.

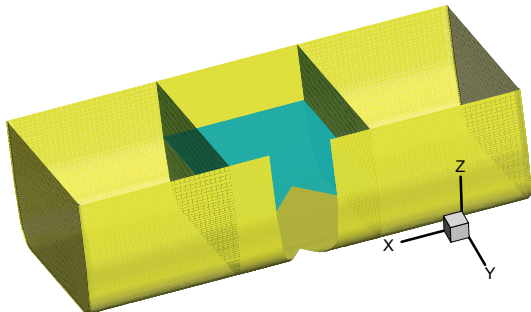


Fig. 4: Sketch of Burgundy model

Table 1: Main dimensions of Burgundy model

Dimension	Intact	damage	intact	damage
Length (m)	60.00	60.00	1.50	1.50
Breadth (m)	27.80	27.80	0.695	0.695
Depth (m)	16.00	16.00	0.40	0.40
Draught (m)	6.25	6.25	0.15625	0.15625
KMT (m)	13.701	13.701	0.3425	0.3425
GMT (m)	0.809	-	0.0202	-
KGT (m)	12.892	-	0.3223	-
Length of Damage (m)	19.20	19.20	0.48	0.48
Δ	9795.2	6660.7	153.05	104.07

The test cases are listed in table 2.

Table 2: Burgundy test cases

Number	Damage	Sway	KG(m)	Roll (°)
1	No	No	0.208	5
2	No	No	0.17	5
3	Yes	Yes	0.208	+5
4	Yes	Yes	0.208	-5
5	Yes	No	0.208	+5
6	Yes	No	0.208	-5

Results and analysis

The computed force components in Case 1 (intact condition) are shown in Figure 5 where K_f , K_p and K_s stands for friction, pressure and hydrostatic forces. It can be seen that the friction force is small compared with pressure force. The hydrodynamic force can be obtained by removing hydrostatic force from total force. It can be seen that hydrostatic force is large and needs to be extracted accurately to derive hydrodynamic coefficients. The comparison of roll decay history in Cases 1 and 2 (intact conditions) is given in Figure 6.

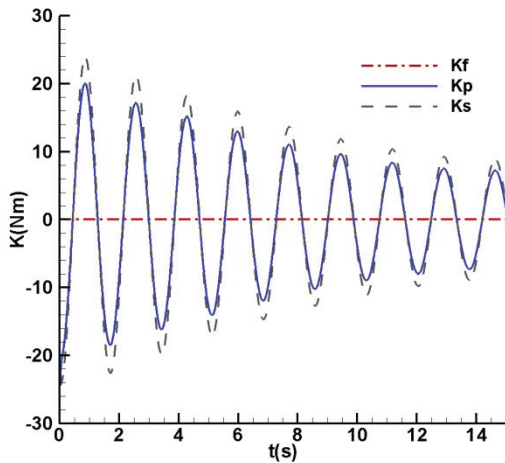


Fig. 5: Moment components

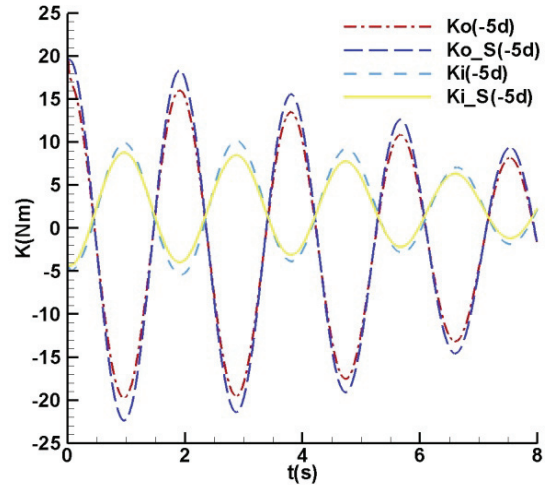


Fig. 7: Moment components

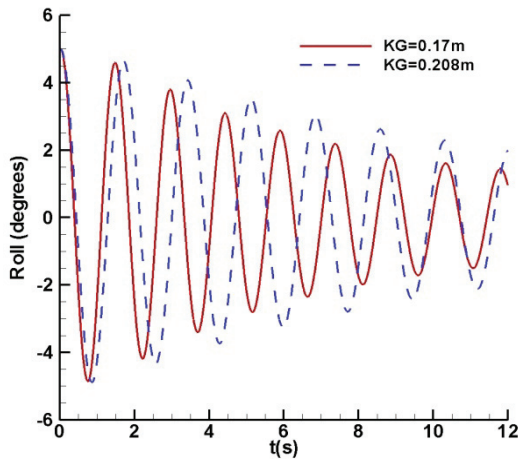


Fig. 6: KG effects on roll decay

It can be seen from Figure 6 that the period decreases slightly with GM increase and roll decay is quicker. Accordingly, the damping increases but added mass decreases.

The fluid loads in the compartment and on the hull in case 4 (damage condition) are shown in Figure 7, where subscript o, i, and s stands for hull, compartment and hydrostatics. Initial heel angle -5 degrees means roll opposite to damage side. It can be seen that hydrodynamic roll moments have nearly 180 degrees phase difference with total hydrostatic force in the tank and on the hull. The total hydrostatic roll moment in damage condition decreases from that in intact condition due to flooding; however, total hydrodynamic force increases. The roll and sway history in case 3 is shown in Figure 8.

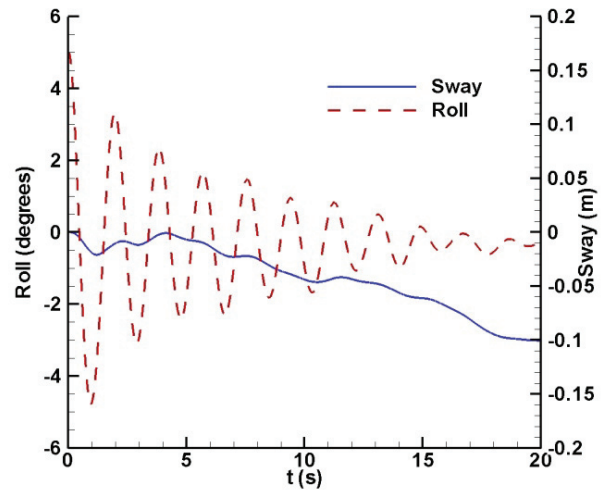


Fig. 8: Roll and sway

It can be seen that there is a sway motion towards undamaged side accompanying roll motion. The computational results from case 3 and 5 in Figure 9 show that there is large difference of roll behavior with and without sway. The sway restricted roll decay tends to increase damping significantly compared to free sway. It indicates that forced roll motions with and without sway will give different damping coefficients.

Additionally, initial roll angle ($+5^\circ$ and -5°) in damage conditions will also affect damping largely as initial heel on damage side ($+5^\circ$) will produce larger hydrodynamic damping than on undamaged side (-5°).

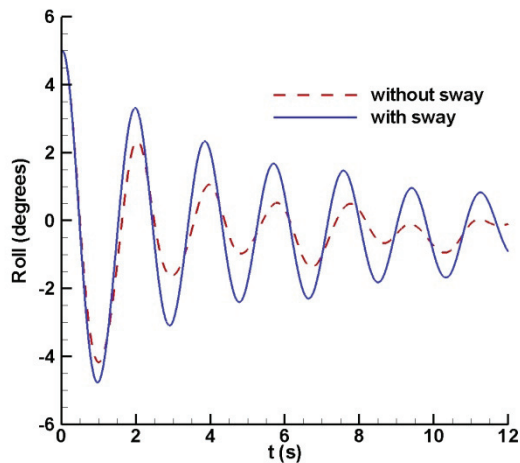


Fig. 9: Sway effect

The computed roll decay histories are processed to obtain hydrodynamic coefficients as shown in Figure 10-12.

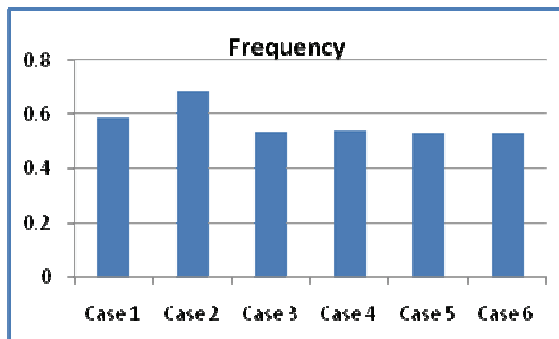


Fig. 10: Natural roll frequency

The roll natural frequency is mostly GM determined. Among 6 test cases, case 2 has larger GM which gives larger frequency. Other 5 cases have the same GM, but the frequency in intact condition is slightly larger than damage condition due to effects of added inertial and damping coefficients.

The results of A44 in Figure 11 show that A44 with larger GM in case 2 is smaller than that in case 1. A44 in damage condition is much larger than that in intact condition due to sloshing in the tank.

The results of B44 in Figure 12 show that B44 with larger GM in case 2 is larger than that in case 1. B44 in damage condition is larger than that in intact condition. It can be seen that B44 without sway (case 5, 6) is much larger than that with free

sway (case 3, 4) and B44 with initial heel on damage side (case 3, 5) is larger than that initial heel on undamage side (4, 6) due to flooding effects. The maximum damping in case 5 (without sway, heel on damage side) is roughly 6 times as large as in case 1 (intact condition).

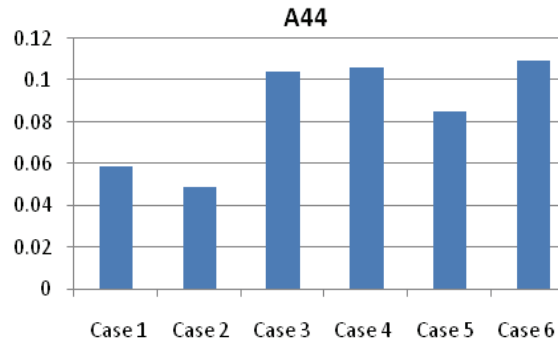


Fig. 11: Case study of A44

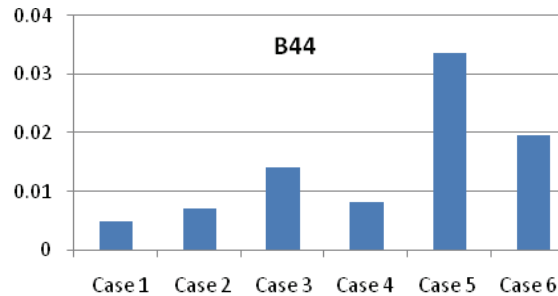


Fig. 12: Case study of B44

The numerical results indicate the different damping characteristics can be obtained by using different methods of model tests.

CONCLUSIONS

The numerical simulations of roll decay were carried out by RANS methods. Based on the results, the following conclusions are drawn:

- The validations of test case DTMB5415 in roll decay show that numerical results of roll decay history and velocity contour agree reasonably well with experiment data. RANS method can be applied to predict roll decay of practical hull form with bulbous bow, transom and bilge keel.
- The GM value has large influence on roll decay behavior, such as roll natural frequency,

added moment of inertia and damping coefficient.

- Sway motion has large effect on hydrodynamic coefficients in damage condition. Added moment of inertia and damping from roll decay without sway are significantly larger than those from roll decay with sway.
- The initial heel angle in damage condition affects the hydrodynamic coefficients notably.

ACKNOWLEDGMENTS

The authors acknowledge and appreciate the travel support offered by the AuxNavalia project (www.auxnavalia.org), which is funded by the Transnational Cooperation in the European Atlantic Area (www.coop-atlantico.com).

REFERENCES

- Irvine, M., Longo, J., Stern, F. (2004), "Towing Tank Tests for Surface Combatant for Free Roll Decay and Coupled Pitch and Heave Motions," Proc. 25th Symp. on Naval Hydrodynamics, St Johns, Canada.
- Mirfield, M., (2001), "Burgundy 2-D forced motion experiment", SSRC internal report
- Wilson R. and Stern F., (2002), "Unsteady RANS Simulation of a Surface Combatant with Roll Motion", 24th Symp on Naval Hydrodynamics, Fukuoka, Japan.
- Gao Q, Jin W. and Vassalos D. (2010), "Simulation of roll decay by RANS approach", Gothenburg CFD Workshop, Sweden